Optimization of melt spun RE-Fe-B powder composition for fully dense, high energy magnets

D. N. Brown,[a] Y. K. Lim, R. A. Remoroza, and D. J. Miller
Magnequench Technology Centre, 01-19 The Galen, 61 Science Park Road, Singapore 117525, Singapore

(Presented 18 November 2010; received 28 September 2010; accepted 21 December 2010; published online 11 April 2011)

Nanocrystalline melt-spun (Nd,Pr)-Fe-B powder can be consolidated into fully dense, anisotropic high-energy magnets by a series of thermo-mechanical processes. The powder composition and processing parameters dictate the magnetic properties of the resulting magnet. More specifically, the alloy must contain a high proportion of the $(Nd,Pr)_2Fe_{14}B$ phase for magnetic performance together with a sufficient grain boundary phase to facilitate the grain alignment mechanism during die-upsetting. This paper demonstrates that the type of rare earth component (Nd,Pr) and minor alloy additions (Cu,Ga) have a dramatic effect on the grain boundary phase and ultimately the magnetic properties. A relatively low cost Pr-Fe-B-Cu alloy has been shown to have enhanced room temperature magnetic performance. However, these advantages are offset by the Pr-Fe-B composition having a larger thermal coefficient of H_{ci} and as a result this type of magnet has inferior performance at 180 °C. © *2011 American Institute of Physics*. [doi:10.1063/1.3564969]

I. INTRODUCTION

Nanocrystalline hot-deformed rare earth permanent magnets are one class of commercially available, fully dense, high strength magnet.[1,2] Such magnets do not have the prominence of sintered Nd-Fe-B magnets[3] but do have some unique and attractive attributes, particularly in the form of ring magnets. Hot-deformed ring magnets are near net-shape formed and have a preferred magnetic orientation in the radial direction. Such magnets are produced in a wide range of sizes [outside diameters (ODs) from 5 mm, height up to 80 mm, and wall thickness ≥ 1 mm], and have relatively low thermal flux loss and excellent corrosion resistance. These features have resulted in hot-worked ring magnets being used in a number of applications from micromotors to automotive power-steering devices.[4–6]

With an increasing number of automotive applications available for permanent magnets, metallurgical developments have focused on reducing cost and improving magnetic performance. Primarily this has meant (i) maximizing B_r and $(BH)_{max}$, (ii) minimizing costly material components like Dy, and (iii) maintaining high magnetic performance at evaluated temperatures (~180 °C).

(i) Remanence can be expressed as a function of saturation magnetization (M_s), magnet density over theoretical density (d/d_0), volume fraction of nonmagnetic phases (V_{nonmag}) and the degree of alignment of magnetic phase (f_φ):

$$B_r = M_s * d/d_0 * (1 - V_{nonmag}) * f_\varphi.$$

For hot-deformed magnets the critical factor to maximizing B_r has been to improve the alignment of $Nd_2Fe_{14}B$ grains (f_φ).

(ii) The scarcity of elements like Dy has led to efforts to reduce the amount of this element required in magnets. Dy has been essential to achieve coercivity levels over 1275 kA/m (16 kOe). $Dy_2Fe_{14}B$ has exceptionally high magnetocrystalline anisotropy ($\mu_0 H_A = 15.0$ T) in comparison to $Nd_2Fe_{14}B$ ($\mu_0 H_A = 6.7$ T).[7] As $Pr_2Fe_{14}B$ has a $\mu_0 H_A$ of 8.7 T this study will investigate the effect of replacing Nd with Pr on the H_{ci} of hot-deformed magnets.

(iii) Automotive applications tend to need room temperature coercivity values of over 1600 kA/m (>20 kOe) to maintain acceptable performance up to 180 °C. Traditionally, Dy and grain boundary refining additions like Ga and Co have been used to maximize the hot-deformed magnet H_{ci} and high temperature performance.[4,8]

This study compares hot-deformed magnets of different rare earth components (Nd and Pr) and alloying additions (Cu and Ga).

II EXPERIMENTAL PROCEDURE

A range of (Nd,Pr)-Fe-B-(Cu,Ga) alloys were prepared using an arc-melter. These alloys were then melt-spun into ribbons and crushed to < 400 μm powder. The compositions of the respective powders were analyzed using inductively coupled plasma spectroscopy (ICP). Differential scanning

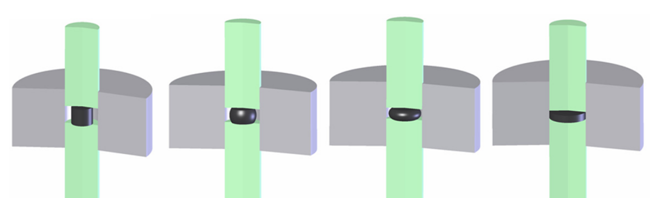

FIG. 1. (Color online) The hot die-upsetting process: A 15 mm-OD fully dense compact is placed in a 25 mm-OD die at ~750 °C. The punches are drawn together and the compact flows outwards until it contacts the die wall.

[a]Author to whom correspondence should be addressed. Electronic mail: dbrown@magnequench.com.

 © 2011 American Institute of Physics

Author complimentary copy. Redistribution subject to AIP license or copyright, see http://jap.aip.org/jap/copyright.jsp

TABLE I. Sample compositions and grain boundary phase melting temperatures.

Sample	Nd	Pr	Fe	B	Ga	Cu	Approximate Grain Boundary Melting Point (°C)
(NdPr)FeB	22.75	7.18	68.94	0.95	—	—	680
(NdPr)FeB-Ga	22.53	7.44	68.37	0.97	0.5	—	585
(NdPr)FeB-Cu	22.35	7.41	68.64	0.92	—	0.48	495
NdFeB-Cu	29.37	0.31	68.74	0.94	—	0.48	508
PrFeB-Cu	0.26	29.05	69.04	0.90	—	0.52	464

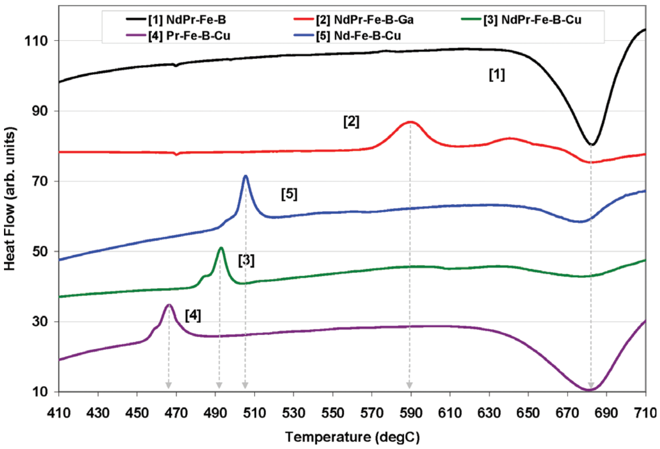

FIG. 2. (Color online) DSC scans of alloy samples.

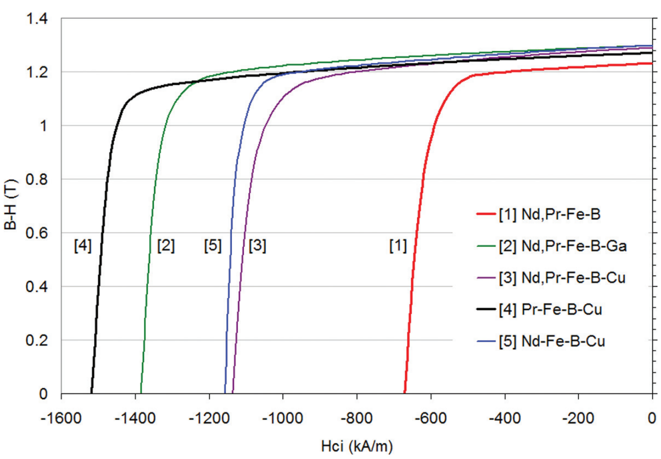

FIG. 3. (Color online) Second quadrant demagnetization curves of hot-deformed samples.

TABLE II. Room temperature magnetic properties of hot-deformed samples.

Sample	B_r(T)	H_{ci}(kA/m)	BH_{max}(kJ/m^3)
(NdPr)FeB	1.23	677	282
(NdPr)FeBGa	1.30	1370	319
(NdPr)FeBCu	1.30	1130	310
NdFeB-Cu	1.30	1162	317
PrFeB-Cu	1.27	1512	306

calorimetry (DSC) was used to identify the grain boundary melting temperatures of the samples.

Hot die-upset disk magnets were then prepared from the powders. Initially 18 g of powder were cold pressed into a 5.5 g/cm^3 dense compact. The compact was then coated in a lubricant and hot pressed to 7.5 g/cm^3 density. These fully dense compacts were then die-upset at approximately 750 °C in a 25 mm diameter die, as illustrated in Fig. 1. The hot pressed parts underwent an approximate 60% height reduction, or 60% surface area increase when die-upset.

Samples of 9.8 × 9.8 mm^2 were wire cut from the center of the die-upset discs, pulse magnetized with 5 T, and measured in a KJS 7000 Hysteresisgraph. A specially constructed coil-set and temperature stage was used in the Hysteresisgraph to measure magnetic properties at elevated temperatures of 100 °C and 180 °C.

The grain size was observed from the fractured magnet surfaces using a Joel JSM-6360LA SEM.

III. RESULTS

Table I presents the ICP measured compositions of the magnets under investigation. This table also lists approximate grain boundary melting temperatures extrapolated from the DSC scans illustrated in Fig. 2. The grain boundary phase melting temperatures are indicated by perturbations in the DSC scans between 450 and 700 °C. The Pr-Fe-B-Cu alloy appears to have the lowest boundary melting temperature, indicated by the endotherm at 464 °C. This implies that the Pr-Fe-B-Cu alloy can be hot-deformed at lower temperatures than the other compositions, and has a longer and more favorable period in which the $Pr_2Fe_{14}B$ grains have to align.

Figure 3 and Table II illustrate the room temperature magnetic properties measured from the hot-deformed magnet samples. The basic (Nd,Pr)-Fe-B alloy has a lower magnetic performance than the other compositions, indicating the importance of small alloy additions like Ga or Cu. The combination of Cu with the Pr-Fe-B alloy is particularly effective at increasing the room temperature H_{ci} value.

Table III and Fig. 4 detail the magnetic properties of (Nd,Pr)-Fe-B-Cu and Pr-Fe-B-Cu over a range of temperatures. Despite having higher room temperature, $H_{ci,}$ the Pr-Fe-B-Cu magnet has a larger thermal coefficient of H_{ci} (> −0.55%/ °C), and this magnet is left with a lower H_{ci} at 180 °C than the (Nd,Pr)-Fe-B-Cu magnet.

Figure 5 illustrates high resolution SEM images of magnet fracture surfaces from the (Nd,Pr)-Fe-B and Pr-Fe-B-Cu samples. No significant difference between the two structures was detected from these images. However, in general,

Author complimentary copy. Redistribution subject to AIP license or copyright, see http://jap.aip.org/jap/copyright.jsp

TABLE III. Magnetic properties of (Nd,Pr)-Fe-B-Cu and Pr-Fe-B-Cu samples at 25, 100, and 180 °C. The thermal coefficient of H_{ci} was calculated between 25–180 °C.

	25 °C			100 °C			180 °C			Thermal coefficient of
Sample	B_r (T)	H_{ci} (kA/m)	BH_{max} (kJ/m^3)	B_r (T)	H_{ci} (kA/m)	BH_{max} (kJ/m^3)	B_r (T)	H_{ci} (kA/m)	BH_{max} (kJ/m^3)	H_{ci} (%/°C)
NdPrFeB-Cu	1.30	1130	310	1.18	567	257	1.01	221	126	−0.52
PrFeB-Cu	1.27	1512	306	1.14	701	244	9.6	215	117	−0.55

there appeared to be more large grains in the (Nd,Pr)-Fe-B sample, as seen in the lower right of the image in Fig. 5(a). These larger, mis-orientated grains will cause a decrease in the magnetic performance.

IV. DISCUSSION

From these results it is clear that both Ga and Cu improved the magnetic properties of hot-deformed magnets. This has been reported before for hot-worked melt-spun material[4,8] and alloy ingots.[9–11] However, observing such a large improvement in H_{ci} with a Pr-Fe-B-Cu hot-worked magnet is novel.

The H_{ci} enhancement is due to a combination of: (i) the higher H_A of $Pr_2Fe_{14}B$ over $Nd_2Fe_{14}B$[7] and (ii) a modification of the grain boundary phase which provides greater resistance to domain movement.

Figures 3 and 4 show the Pr-Fe-B-Cu magnets to have particularly square second quadrant demagnetization curves, which indicate a high degree of $Pr_2Fe_{14}B$ grain alignment. This can be attributed to the low melting point grain boundary phase providing more favorable grain aligning conditions during the hot die-upsetting process.

The initial benefits of high H_{ci}, strong grain alignment, and a low cost alloy formulation seen with the Pr-Fe-B-Cu sample are offset by the rather disappointing high temperature performance (Fig. 4). The $Pr_2Fe_{14}B$ phase appears to be less suitable for high temperature applications than the $Nd_2Fe_{14}B$ phase.

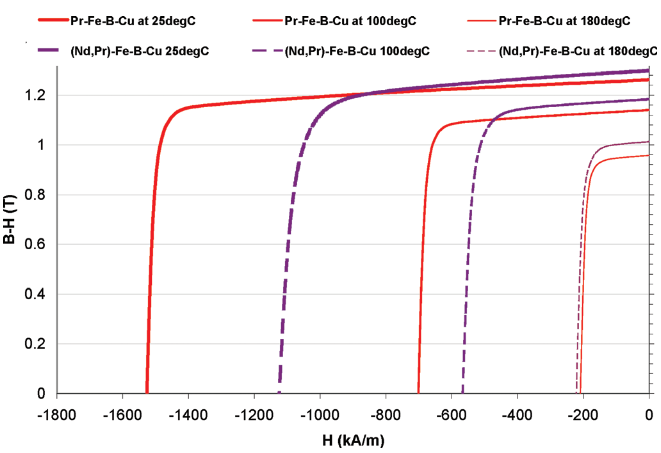

FIG. 4. (Color online) Second quadrant demagnetization curves of (Nd,Pr)-Fe-B-Cu and Pr-Fe-B-Cu magnets at 25, 100, and 180 °C.

V. CONCLUSION

Hot-deformed magnets prepared from melt-spun Pr-Fe-B-Cu exhibit a high degree of grain alignment, high room temperature H_{ci}, and use relatively inexpensive elements.

The Pr-Fe-B-Cu composition has a low melting point grain boundary phase, which is favorable for the die-upsetting process.

The drawback with the Pr-Fe-B-Cu sample is that it has a large thermal coefficient of H_{ci} and any magnetic performance advantage is lost at elevated temperatures around 180 °C.

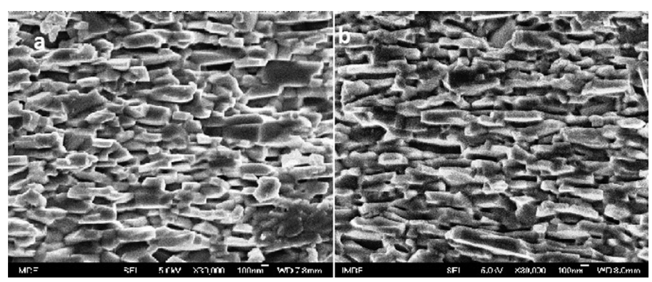

FIG. 5. High resolution SEM images of fracture surfaces from (a) (Nd,Pr)-Fe-B and (b) Pr-Fe-B-Cu magnet samples.

[1] R. W. Lee, Appl. Phys. Lett. **46**, 790 (1985).
[2] C. D. Fuerst, E. G. Brewer, R. K. Mishra, Y. Zhu, and D. O. Welch, J. Appl. Phys. **75**, 4208 (1994).
[3] M. Sagawa, S. Fujimura, M. Togawa, H. Yamamoto, and Y. Matsuura, J. Appl. Phys. **55**, 2083 (1984).
[4] N. Yoshikawa, T. Iriyama, H. Yamada, Y. Kasai, and V. Panchanathan, IEEE Trans. Magn. **35**, 3268 (1999).
[5] N. Yoshida, Y. Kasai, T. Watanabe, S. Shibata, V. Panchanathan, and J. J. Croat, J. Appl. Phys. **69**, 6049 (1991).
[6] http://www.daido-electronics.co.jp/english/product/neoquench_dr/index.html
[7] K. H. J. Buschow, Rep.Prog. Phys. **54**, 1123 (1991).
[8] A. Kirchner, D. Hinz, V. Panchanathan, O. Gutfleisch, K. H. Müller, and L. Schultz, IEEE Trans. Magn. **36**, 3288 (2000).
[9] T. Shimoda, K. Aioka, O. Kobayashi, T. Yamagami, T. Ohki, M. Miyagawa, and T. Yuri, IEEE Trans. Magn. **25**, 4099 (1989).
[10] Z. Chen, Z. Shi, L. Wang, and H. Fu, J. Appl. Phys. **71**, 2799 (1992).
[11] G. P. Hatch, A. J. Williams, G. J. Mycock, and I. R. Harris, J. Magn. Magn. Mater. **157**, 69 (1996).

Author complimentary copy. Redistribution subject to AIP license or copyright, see http://jap.aip.org/jap/copyright.jsp